DECENTRALIZED GRID CONTROL USING POWER GRID STATE ESTIMATION

Eberhard WAFFENSCHMIDT
TH-Köln, Germany
eberhard.waffenschmidt@th-koeln.de

Markus DE KOSTER
TH-Köln, Germany
markus.de_koster@smail.th-koeln.de

Christian HOTZ
TH-Köln, Germany
chritian.hotz@th-koeln.de

Sergej BAUM
TH-Köln, Germany
sergej.baum@th-koeln.de

Ingo STADLER
TH-Köln, Germany
ingo.stadler@th-koeln.de

ABSTRACT

A decentralized power grid control using a Swarm-Grid approach is proposed. It includes an exchange of measured data between components and a grid state estimation. Here, methods for calculating the current grid state and for generating pseudo measurements in case of non-convergence of the algorithm are proposed. Additionally, worst-case assumptions are presented which help to achieve reasonable estimates of the unknown grid voltages and currents used for the decentralized grid control. Finally the impact of unknown phase information is derived.

INTRODUCTION

Distributed power generation with renewable energies benefits from distributed control of power distribution. The concept of cellular grids [1] proposes a distributed power grid structure for this purpose. Thus, a proposal is made for the control of such a cellular power grid structure, which is called "Swarm Grid" by the authors [2]. The name refers to the swarm-like control structure that does not require a higher-level controller to coordinate the grid components.
This publication explains the concept of such a swarm grid in the first chapter. Charging stations for electric vehicles as the background of this use case are presented as exemplary grid components. Therefore, in the further course of this publication, charging stations are to be considered synonymous with controllable loads.
The "Swarm Grid" approach includes the estimation of the grid state from commonly exchanged measured data. Therefore, the following chapter shows details on the used methods for the grid state estimation. If insufficient known values are available for the algorithm to converge a suitable solution, strategies are necessary to either increase or decimate the number of unknown values. They are based on the side condition that the worst case must be covered.
As one further problem, in many cases the phase information of voltages and currents are lacking, which leads to estimation error of the line currents. This is investigated in the last chapter.

SWARM GRID

In a swarm (e.g. a school of fish), members are able to measure (e.g. fish can see), know about or communicate with each other (e.g. keep an eye on each other), decide and react (e.g. change swimming direction). Similarly, the components in a swarm grid should be able to measure, communicate with each other, process the information and react. Specifically, the concept presented includes the following:
The components are able to measure the voltage at the connection point and the power or current of the device connected to that point. In a more advanced environment, the devices are able to measure the voltage angle or even the mains impedance. The components communicate with each other by exchanging the measured information (see illustration in Figure 1). In this way, each component can get an overview of a much larger part of the network than just the connection point. Preferably, the communication is based on powerline communication, so that only components in the same network branch communicate with each other.
Considering the measured values, each grid component is able to calculate a detailed picture of the current network status. From these calculations, the components can make decisions about their behaviour, e.g. power management to avoid overload. Based on this information, an optimization of the charging process can be derived [3].
By its very nature, this only applies to controllable loads whose output can be modulated without significantly affecting their function. This can apply to components such as charging boxes for electric vehicles, electric heat pumps, air conditioning controls, batteries or combined heat and power (CHP) systems. Such components will dominate future distribution grids in a 100 % renewable energy society.

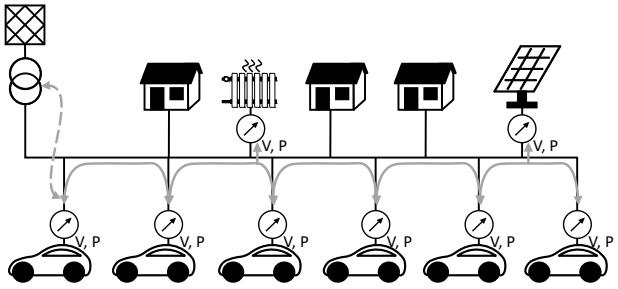

Figure 1: Illustration of decentralised grid control based on the swarm principle.

STATE ESTIMATION

Fundamentals

An overview of existing distribution system state estimation (DSSE) approaches is given in [4]. All approaches have in common that the calculation is

performed by the Distribution System Operator (DSO) that then decides on which actions to take to ensure a stable operation.
In this paper, performing DSSE on distributed nodes is proposed. Because of that, the availability of data greatly differs. While in centralised DSSE measurements from Smart Meters are available to the DSO, data protection laws inhibit the ability to share user specific data especially in countries with strict data protection laws such as Germany.
Furthermore, our application for grid control requires that the worst case for the grid state must be covered. This is different from applications, which analyse the system state for purposes such as fault localisation or loss monitoring [4].
In traditional state estimation, a state vector is built with either node voltages, branch currents or power. Notably, one vector needs to be complete in order for the algorithms such as Weighted Least Squares (WLS) to work. Therefore, if no measurement value is available for a node or branch, replacement values have to be used instead.[10]

Replacement Values

Existing algorithms require a positive measurement value redundancy at each node (η_{local}) and for the whole low voltage network(η_{global}) [10]. However, in reality, it is expected that the number of unknown values is significantly higher than amount of available measurements.
As a solution, unknown values can be replaced by replacement values. There exist two types of replacement values, virtual measurements and pseudo measurements.
Virtual measurements are those that for simulation purposes show no measurement error such as current values for nodes without energy consumption or production, often called Zero Injection Busses (ZIB) [8].
Pseudo measurements can be generated through statistical and probalistical algorithms such as Gaussian Mixture Models or Expectation Maximization, through learning based algorithms such as deep neural networks (DNN) or Parallel Distribution Processing (PDP) based on historical data [4].
If there is an excess of unknown values, one has to select, whether a value is put into the batch of those, that will be calculated from the measurements, or whether it will be set to a pseudo or virtual measurement value.
Even, if the process of selection is often clear to a skilled user, it is not always straightforward for an automated process. It will be described in the following chapter.

Notation and preliminaries

Nodes will be referred to as *measurement busses*, if – at that node – measurements are taken, as *estimation busses* if its values are calculated and lastly as *zero injection busses* if virtual measurements are applied.
The grid topology is assumed to be known either through manual input or through topology estimation. Thus, also the admittance matrix is available.
Further, the grid topology contains information about whether a node is capable of feeding into the network.
In a first iteration, only radial networks are considered. However, the algorithm can also be applied to meshed networks.
For simulation purposes, grid topologies were generated in form of binary trees with restrictions that measurement busses may only be at the end of a line and estimation busses only at the end of a line or immediately before measurement busses. This shall represent public and private electric vehicle charging stations, and households.
Finally, the phase shift at a slack node is assumed to be known (typically zero).

Algorithm

In the proposed algorithm of this paper, a combination of node voltages and branch currents can be used as the state vector. With only a limited number of known values, the voltage and current vectors each are incomplete. A model-based approach is used for DSSE.
Equation (1) shows the matrix form of Ohm's Law for a single phase, symmetrical system, where $\vec{I}$ are all node currents, $\vec{U}$ are the node voltages and A is the admittance matrix which interlinks known node voltage with unknown node currents:

$$\vec{U} * A = \vec{I} \tag{1}$$

In our case, however, not all node voltages are known, and some of the node currents are already known.
To solve this problem, rows can be extracted from equation (1) resulting in equation (2), where δ, β are those row indices of known values in $\vec{U}$, $\vec{I}$ and $\bar{\delta}$, $\bar{\beta}$ row indices of unknown values in $\vec{U}$, $\vec{I}$ respectively.

$$A[\beta,\delta]\cdot\vec{U}[\delta]-\vec{I}[\beta]=-A[\beta,\bar{\delta}]\cdot\vec{U}[\bar{\delta}] \tag{2}$$

This results in a linear equation system with only known values on the left and part of the admittance matrix and all unknown values in $\vec{U}$ on the right.
Using WLS the unknown values in $\vec{U}$ can be determined with weights assigned according to measurement accuracies.

Transformation using Principal Pivot Transform

A different approach for calculating unknown values in $\vec{U}$ was evaluated during work on this paper. Here, for those rows with existing current measurement values β and non-existant voltage values $\bar{\delta}$ elements are exchanged between $\vec{U}$ and $\vec{I}$ resulting in two new vectors $\vec{X}$ and $\vec{Y}$. This process also known as *exchange operator* requires transforming the matrix using Principial Pivot Transform (PPT) as shown in equation (3).

$$\vec{Y} * ppt(A,\alpha) = \vec{X} \tag{3}$$

Here, the indices of exchange are noted in α and those that have not been changed are by definition noted in $\bar{\alpha}$. Using these indices four submatrices A[α], A[α, $\bar{\alpha}$], A[$\bar{\alpha}$, α] and A[$\bar{\alpha}$] can be extracted that together form the whole

admittance matrix, where the first parameter is row index and the second parameter column index. If only one parameter is given, row and column index values are identical. Further the Schur Complement A_{Schur} is given as $A[\bar{\alpha}] - A[\bar{\alpha},\alpha] \cdot A[\alpha]^{-1} \cdot A[\alpha,\bar{\alpha}]$

$$\begin{matrix} A[\alpha]^{-1} & -A[\alpha]^{-1} \cdot A[\alpha,\bar{\alpha}] \\ A[\bar{\alpha},\alpha] \cdot A[\alpha]^{-1} & A_{Schur} \end{matrix} \quad (4)$$

The PPT of the matrix A with exchange indices α is defined as ppt(A, α) in equation (4) [5].
As can be seen, PPT requires inversion of the sub-matrix A[α] and thus no linear dependence in this sub-matrix. However singularity in A[α] is unlikely since the submatrix contains the self-admittances on its diagonal. In case of singularity, using a Moore Penrose Inverse is applicable under certain conditions described in equation (5) according to [6]. Here, N(A) is the nullspace of A and A* is the complex conjugate of A.

$$N(A[\alpha]) \subseteq N(A[\bar{\alpha},\alpha]) \quad (5)$$

$$N(A^*[\alpha]) \subseteq N(A^*[\alpha,\bar{\alpha}]) \quad (6)$$

Reference [7] finds a more generalized definition shown in equation (6), where R(A) denotes the range space of A.

$$R(A[\alpha,\bar{\alpha}]) \subseteq R(A[\alpha]) \quad (7)$$

If a pseudo-inverse is used, the transformation is referred to as Generalized Principal Pivot Transform (GPPT).
Then, the matrix can be transformed similar to equation 2 resulting in an equation system with fewer unknowns and fewer equations than in the first approach. However, in both approaches all measurement values are used and after applying WLS both result in similar results for the voltage Vector.

Constrained Least Squares

With the fully calculated voltage vector and the complete admittance matrix, the current vector can also be calculated. Therefore, a Constrained Least Squares algorithm (CLS) with addition of boundaries is used. A review on constrained state estimation algorithms can be found in [11].
Since the transformer is included in the distribution system all currents must add up to 0. Thus, this information was used as a constraint with an added margin of 2%. Using the available information obtained from grid topology about which bus is capable of feeding into the system, an upper boundary of I = 0 was set for those nodes. Further, for ZIB lower and upper boundary were set to I = 0.Then, we minimize the euclidean 2-norm $\left\| A * \vec{U} = \vec{I} \right\|_2$. In case the results did not converge to a feasible solution, methods were applied to reduce the amount of unknown values as described in the following section

Worst-case scenarios

In general, those grid topologies posed problematic to the algorithm that showed a lack of measurements in close proximity and especially towards the end of the power line.

In order to decrease the amount of unknown values, estimation busses were converted to ZIB with an assumed active current of zero. To ensure grid stability the nodes were converted in such a way that a worst-case topology is generated. This was achieved by first identifying the estimation node that showed the highest divergence from the expected value. Then, starting with the identified node and moving on the line directly towards the transformer the last estimation node before the nearest measurement node was converted to a ZIB.

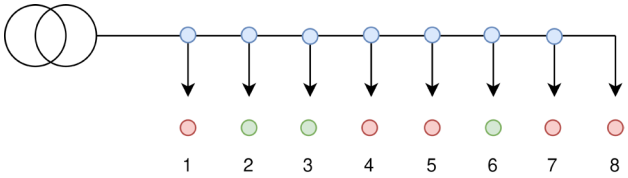

Figure 2: Exemplary Grid Topology with estimation nodes marked as red, measurement nodes as green and blind nodes as blue

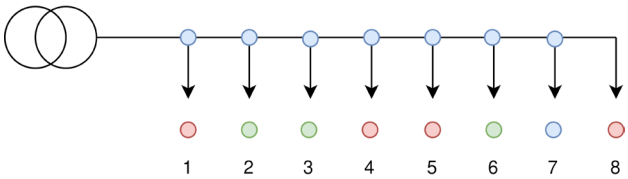

Figure 3: Exemplary Grid Topology with converted node

This way, the algorithm assumes currents of the converted nodes must be assigned to the node furthest away from the transformer. This is defined as the worst case scenario since it results in the highest possible voltage drop and line currents.
Figure 2 shows an exemplary radial grid topology with only one main branch. Assuming the highest divergence from the expected value occurred in node 8, according to the proposed worst-case assumption, node 7 is converted as shown in Figure 3.

Results

Figure 5 compares results of the state estimation to actual values as extracted from the simulation environment. As can be seen, for lower ratios of estimation busses to measurement busses the estimation is highly accurate. Even though the accuracy decreases with more estimation busses compared to measurement busses and thus fewer known values, the results are still fairly accurate with an error below 0.15% as a maximum deviation.
It shall be noted that the worst case strategies were only employed if the voltage deviated more than 20 V from 230 V. This strategy results in outliers in simulation data as can be seen for ratio 0.3 and 2.0. To tackle this issue, an exhaustive search for the optimal solution may be used in future work at the cost of additional computational complexity. Further, the difference from expected values accurately reflects worst case scenarios as the voltage deviates in negative direction resulting in higher calculated voltage drops than actually exist. Only few cases existed where the voltage difference was positive.

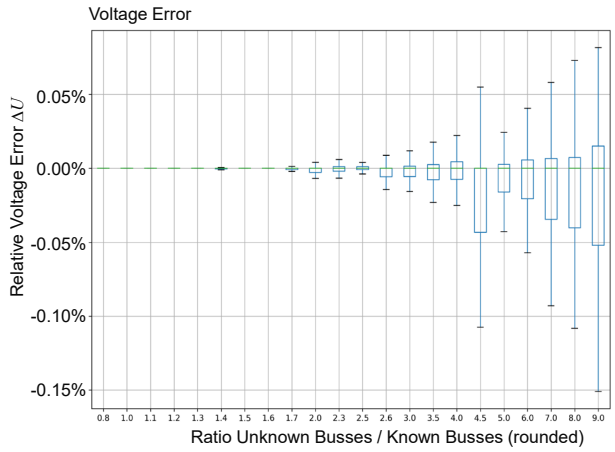

Figure 4: Difference between expected and calculated values over ratio between amount of estimation to measurement busses.

Notably, due to the simulation setup not all ratios are represented equally.

Possible Improvements

Using a symmetric simplified equivalent network for low voltage systems that are mostly operated asymmetrically may result in increased errors [8]. Because of that, the calculation can be performed using symmetric components.

In addition, the proposed algorithms need to be compared to traditional algorithms in regards to performance and accuracy. Further, estimation and measurement nodes were assigned fixed values that did not alternate throughout the simulation. Instead, load profiles should be used in future work.

Finally, the proposed algorithm should be tested outside of simulations and in varying scenarios.

INFLUENCE OF VOLTAGE PHASOR

As one further problem, in many cases the phase information of voltages and currents are lacking, which leads to estimation error of the line currents. This is investigated in the following section. Similar results have been published in German as part of a conference contribution before [9].

First, the voltage difference $\Delta\underline{U}_L$ between two nodes with known node voltages $\underline{U}_1$ and $\underline{U}_2$ in a network branch is considered. Using Ohm's law the line current connecting the two nodes can be calculated. The lines are each modelled with resistance R_L and inductive reactance X_L.

With this arrangement, the pointer diagram of the voltages in the complex plane Figure 5 is derived. The voltage U_2 is assumed being real and the unknown line current I_L is generally assumed being a complex current, consisting of the real part I_P and the imaginary part I_Q.

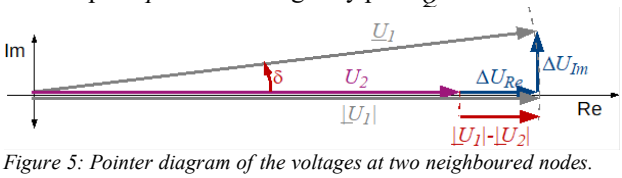

Figure 5: Pointer diagram of the voltages at two neighboured nodes.

The difference in the voltage magnitudes is almost equal to the real part of the complex voltage $\Delta\underline{U}_{Re}$ across the line. In the following, this quantity will be referred to as ΔU (without underscore):

$$|U_1| - |U_2| = \Delta U \approx \Delta U_{\mathrm{Re}} = I_P \cdot R_L - I_Q \cdot X_L \qquad (8)$$

If no phase information were available, the assumption would be made that the line current is purely real. This is taken as calculated reference. Then, the following line current I_{Lest} is estimated:

$$I_{Lest} \approx \Delta U / R_L \qquad (9)$$

However, as soon as the line current I_L has a reactive current component I_Q, an error appears. Equation (8) applies to ΔU and what really is calculated with the previous assumption is:

$$I_{Lest} \approx \frac{I_P \cdot R_L - I_Q \cdot X_L}{R_L} = I_P - I_Q \cdot \frac{X_L}{R_L} \qquad (10)$$

Considering the absolute value of the current $|I_L|$ being calculated by Pythagoras from I_P and I_Q, the current I_P can be replaced:

$$I_{Lest} \approx \sqrt{|I_L{}^2| - I_Q^2} - I_Q \cdot \frac{X_L}{R_L} \qquad (11)$$

Related to the line current I_L, this gives:

$$\frac{I_{Lest}}{|I_L|} \approx \sqrt{1 - \left(\frac{I_Q}{|I_L|}\right)^2} - \frac{I_Q}{|I_L|} \cdot \frac{X_L}{R_L} \qquad (12)$$

We define a reactive power factor $QF = -I_Q/|I_L|$ for the line current, analogous to the power factor PF (also cosφ). As an advantage, its sign indicates the type of reactive power. This gives the relative estimated line current:

$$\frac{I_{Lest}}{|I_L|} \approx \sqrt{1 - QF^2} + QF \cdot \frac{X_L}{R_L} \qquad (13)$$

Figure 6 shows the relative estimated line current I_{est} as a function of the reactive power factor QF according to equation (13). The reactive resistance ratio of the line X_L/R_L is varied as a parameter.

To explain the curves one recognises two terms in equation (13) that contribute to the error. The term under the root describes the error contribution of the reactive current. This share is visible in the curve for $X_L/R_L = 0$ (green). It is symmetrical to the zero point due to the square in the term. It leads to a systematic underestimation of the actual flowing current.

The second term contains an additional error due to the inductive component of the line. It is not symmetrical and leads to an overestimation for an inductive component of the line current and an underestimation for a capacitive component. In the inductive range, this term partially compensates for the error due to the first term. The second term still contains the reactive power factor, which is assumed unknown here. Therefore, the second term cannot be calculated out, even if both real resistance and reactive resistance of the line are known.

Although very large errors occur in Figure 6, these deviations can be relativized in practice. Especially in the low-voltage grid, the share of the line's reactance is comparatively small. As two typical examples, a cable type VPE4x150SE-400V has an impedance ratio of X_L/R_L

= 0.5 and an overhead line A50-400V has an impedance ratio of X_L/R_L = 0.5. This corresponds to the dark yellow as well as the light orange curve. This is in the area, where the two error terms compensate each other and the values deviates by a maximum of around 10%.
Since this deviation also provides a larger estimated value, the deviation is on the safe side for the application. Capacitive line currents, on the other hand, occur mainly in low-load cases due to cable capacitance and are then low. Therefore, a deviation in this range is less critical.
However, in medium and high voltage lines the reactive part of the line impedance becomes more dominant. Then, a simple estimate results in a high error. Therefore, for medium and high voltage grids the measurement of the voltage phase is necessary to be able to calculate completely with complex numbers.

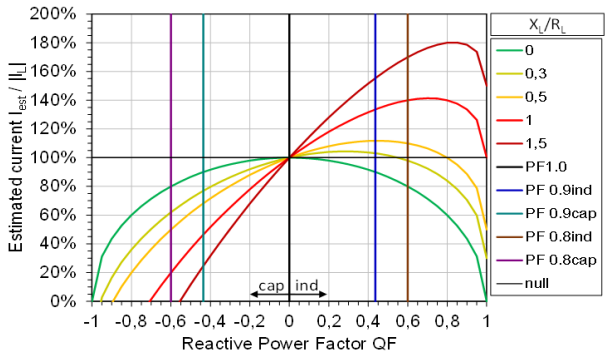

Figure 6: Estimated line current I_{est} related to the actual line current I_L between two nodes as a function of the reactive power factor Q_F of the line current and the ratio X_L/R_L of the line as parameter.

CONCLUSIONS

This paper shows a suitable method to determine the grid state for grid control. Especially the proposed strategies for decreasing the amount of unknown values in worst-case scenarios proved to be successful. Furthermore, it has been shown that for applications in the low voltage grid the missing phase information leads to typically estimation errors I the range of 10%, where the estimation is on the safe side.

ACKNOWLEDGMENTS

This research project has received funding from the Electronic Components and Systems for European Leadership Joint Undertaking under grant agreement No. 876868. This Joint Undertaking receives support from the European Union's Horizon 2020 research and innovation programme and Germany, Netherlands, Spain, Italy, Slovakia.

REFERENCES

[1] J.Bayer, T.Benz, N.Erdmann, F.Grohmann, H.Hoppe-Oehl, J.Hüttenrauch, P.Jahnke, S.Jessenberger, G.Jost, G.Kleineidam, H.Melzer, G.Remmers, S.Rummeny, P.Schegner, H.Schroeder, B.Uhlemeyer, E.Waffenschmidt, M.Zdrallek, „Zellulares Energiesystem - Ein Beitrag zur Konkretisierung des zellularen Ansatzes mit Handlungsempfehlungen“, VDE-Fachbeitrag, Mai 2019

[2] Eberhard Waffenschmidt, "Swarm Grids - Distributed power grid control for distributed renewable power generation", Keynote presentation at 11th International 100% Renewable Energy Conference (IRENEC 2021), 20.-22. May 2021

[3] André Ulrich, Sergej Baum, Ingo Stadler, Eberhard Waffenschmidt, Christian Hotz, "Maximising Distribution Grid Utilisation by Optimising E-Car Charging Using Smart Meter Gateway Data", SDEWES 2022, Paphos, Cyprus, 06.-10.Nov.2022

[4] M. Fotopoulou, S. Petridis, I. Karachalios, and D. Rakopoulos, “A Review on Distribution System State Estimation Algorithms,” en, Applied Sciences, vol. 12, no. 21, p. 11 073, Nov. 2022, ISSN: 2076-3417. DOI: 10 . 3390 / app122111073. [Online]. Available: https : / / www.mdpi.com/2076- 3417/12/21/11073 (visited on 01/03/2023).

[5] M. J. Tsatsomeros, “Principal pivot transforms: Properties and applications,” en, Linear Algebra and its Applications, vol. 307, no. 1-3, pp. 151–165, Mar. 2000, ISSN: 00243795. DOI: 10.1016/S0024-3795(99)00281- 5. [Online]. Available: https://linkinghub.elsevier.com/ retrieve/pii/S0024379599002815 (visited on 10/09/2022).

[6] M. Rajesh Kannan and R. Bapat, “Generalized principal pivot transform,” en, Linear Algebra and its Applications, vol. 454, pp. 49–56, Aug. 2014, ISSN: 00243795. DOI: 10.1016/j.laa.2014.04.015. [Online]. Available: https:// linkinghub.elsevier.com/retrieve/pii/S0024379514002298 (visited on 10/19/2022).

[7] K. Kamaraj, P. S. Johnson, and S. M. Naik, “Generalized principal pivot transform and its inheritance properties,” en, The Journal of Analysis, vol. 30, no. 3, pp. 1241–1256, Sep. 2022, ISSN: 2367-2501. DOI: 10. 1007/s41478-022-00399-w. [Online]. Available: https:/ / doi . org / 10 . 1007 / s41478 - 022 - 00399 - w (visited on 11/02/2022).

[8] R. Brandalik, “Ein Beitrag zur Zustandsschätzung in Niederspannungsnetzen mit niedrigredundanter Messwertaufnahme,”de, p. 223.

[9] Eberhard Waffenschmidt, Christian Hotz, Sergej Baum, Ingo Stadler, "Swarm Grids - Verteilte Stromnetzsteuerung für verteilte erneuerbare Energieerzeugung", Tagung Zukünftige Stromnetze 2022, 26. - 27. Januar 2022, online

[10] D. M. Wäresch, “Entwicklung eines Verfahrens zur dreiphasigen Zustandsschätzung in vermaschten Niederspannungsnetzen,” p. 235.

[11] N. Amor, G. Rasool, and N. C. Bouaynaya, “Constrained State Estimation -- A Review.” arXiv, Mar. 11, 2022.